



This is the author's version of a work that was accepted for publication in the following source:

Payne, S. C., O. Burns, M. J. Stebbing, R. Thomas, A. C. de Silva, A. Sedo, F. Wiessenborn, T. Hyakumura, M. Huynh, C. N. May, R. A. Williams, J. Furness, J. Fallon, and R. Shepherd. 2019. Vagus nerve stimulation to treat inflammatory bowel disease: a chronic, preclinical safety study in sheep. *Bioelectronics in Medicine*. **1**(4): 235-250.

doi: <https://doi.org/10.2217/bem-2018-0011>

Notice: Changes introduced as a result of publishing processes such as copy-editing and formatting may not be reflected in this document. For a definitive version of this work, please refer to the published source.

The final publication is available [here](#)

Copyright of this article belongs to: © 2018 Future Medicine Ltd

40 3. * Martelli et al., 2014. *Auton. Neurosci.* This paper reviews the mechanisms and
41 experimental evidence of the anti-inflammatory effects of vagal nerve stimulation

42 4. * Tyler and Durand 2003. *Ann. Biomed. Eng.*
43 The design of our electrode array was adapted from the flat interface nerve electrode
44 described in this paper.

45 5. * Hoffman and Schnitzlein 1961. *Anatomical Record*
46 This paper describes the anatomy of the human vagus nerve, including fiber types, in detail.

47 6. * Payne et al., 2018 *Nat. Rev. Gastroenterol & Hepatol.*
48 This paper describes the mechanisms and clinical evidence of the anti-inflammatory effects
49 of vagal nerve stimulation to relieve inflammatory bowel disease

50 **Key words**

51 Inflammatory bowel disease, vagus nerve stimulation, peripheral nerve, electrode array

52

53 **1. Introduction**

54 Neurotechnology has improved the lives of millions of patients worldwide *via* the
55 stimulation of, or recording from, target neural populations [1]. Neural stimulators
56 provide sensory feedback in deprived systems (deafness), motor control to effect
57 movement disorders (Parkinson's disease), or treatment to relieve disease symptoms
58 (epilepsy) [2]. The peripheral nervous system has extensive, surgically accessible,
59 neural connections with the central nervous system and end organs [3]. A number of
60 peripheral nerve stimulation sites have been utilised for a range of different disorders,
61 including targeting sacral (pelvic) nerves for the treatment of faecal incontinence [4],
62 constipation [5] and urinary dysfunction [6, 7]. Applications for bioelectric
63 neuromodulation of the cervical vagus nerve to treat disease are diverse. Cervical vagus
64 nerve stimulation (VNS) is an FDA approved treatment for epilepsy [8] and depression
65 [9]. Following the discovery that stimulation of the vagus nerve inhibits acute
66 inflammation [10], promising pilot open label clinical studies show that stimulation of
67 the left cervical vagus nerve has therapeutic efficacy in the treatment of inflammatory
68 diseases such as rheumatoid arthritis [11] and inflammatory bowel disease (IBD) [12].
69 However, there are limitations and adverse side effects associated with stimulation of
70 this target. A pivotal efficacy and safety study of left cervical VNS in epileptic patients
71 (n=95) reported that at 3 months post-surgery, 63% of patients had experienced
72 dysphonia, 44% coughing, 37% pain and 24% dyspnea during stimulation [13]. These
73 issues were not resolved after 12 months, with over half of the patients (55%)
74 continuing to experience voice alterations, while 15% of patients still experienced pain,
75 and coughing [14]. Similarly, during an open label pilot clinical trial Crohn's disease
76 patients implanted with a similar device on the left cervical vagus nerve experienced
77 dysphonia [12]. To minimise these off-target effects, the intensity and the duration of
78 stimulation can be reduced; however, this may reduce the therapeutic efficacy.

79

80 Anatomical and physiological studies provide insight into the off-target effects observed
81 during stimulation of the left cervical vagus nerve. The vagus nerve in the cervical
82 region is composed of fast conducting myelinated A- and B-fibers, and slow conducting
83 unmyelinated C-fibers. A- and B-fibers have lower electrical thresholds than the target
84 C-fibers [15]. Electrical activation of slow conducting unmyelinated vagal C-fibers likely
85 drives the anti-inflammatory effects in inflammatory diseases such as rheumatoid
86 arthritis and IBD [16, 17]. Because of their higher thresholds, activation of cervical vagal
87 C-fibers will also activate A-and B-fibers, resulting in off-target effects that have been
88 reported clinically.

89 The left vagus nerve, which is the target site for depression and epilepsy, branches to
90 innervate the larynx, pharynx, heart and lungs. The nerve traverses through the thoracic
91 cavity into the abdominal cavity and becomes what is known as the anterior abdominal
92 vagus nerve, and forms the hepatic, celiac and gastric branches to innervate visceral
93 organs [18]. The anterior abdominal vagus nerve consists of 97% C-fibers [19] and is
94 below vagal branches to the larynx, heart and lungs. Therefore, we hypothesised that
95 stimulating the nerve at this location will reduce the potential off-target affects that are
96 experienced with left cervical VNS.

97 We hypothesised that stimulating the anterior (i.e. left) vagus nerve below branches to
98 the larynx, heart and lungs would result in the recruitment of C-fibers that have anti-
99 inflammatory effects, while minimizing stimulus-induced off-target effects. In order to
100 demonstrate that stimulation levels employed are above C-fiber thresholds, we
101 developed an electrode array with multiple electrode pairs designed to both stimulate
102 and record electrically-evoked neural activity. In order to improve neural recordings of
103 C-fibers, the cuff electrodes were designed to reshape the nerve slightly for an optimal
104 electrode-neural interface, similar to methods reported by Tyler and Durand [20].
105 Taken together, we aimed to develop a multi-bipolar cuff electrode array that was able
106 to stimulate and record evoked neural activity.

107 The potential for electrical stimulation-induced tissue damage is a limiting factor when
108 selecting stimulation parameters [21]. The Shannon limit for current intensity describes
109 the boundary between damaging and non-damaging stimulation levels [22-24]. If this
110 limit is exceeded, stimulus-induced neuronal damage can occur due to the production of
111 irreversible electrochemical reactions at the electrode-neural interface. Furthermore,
112 damage from high stimulus intensities can be induced by fatiguing the neurons.
113 Continuous metabolic demands on stimulated neurons may lead to over activation of
114 mitochondria and the generation of free radicals, oxidative stress and tissue damage
115 [25]. Therefore, testing of stimulus regimes using electrode arrays and the target neural
116 population intended for clinical application is essential for the evaluation of safety.

117 Here, we sought to evaluate the safety of chronic implantation and electrical stimulation
118 of the anterior vagus nerve below the branches to the larynx, heart and lungs in a large

119 animal model (sheep). Stimulus parameters well above those required to evoke neural
120 activity were used and the nerve was assessed for changes in function or damage.
121 Moreover, we monitored potential off-target effects of stimulation.

122

123 **2. Methods:**

124

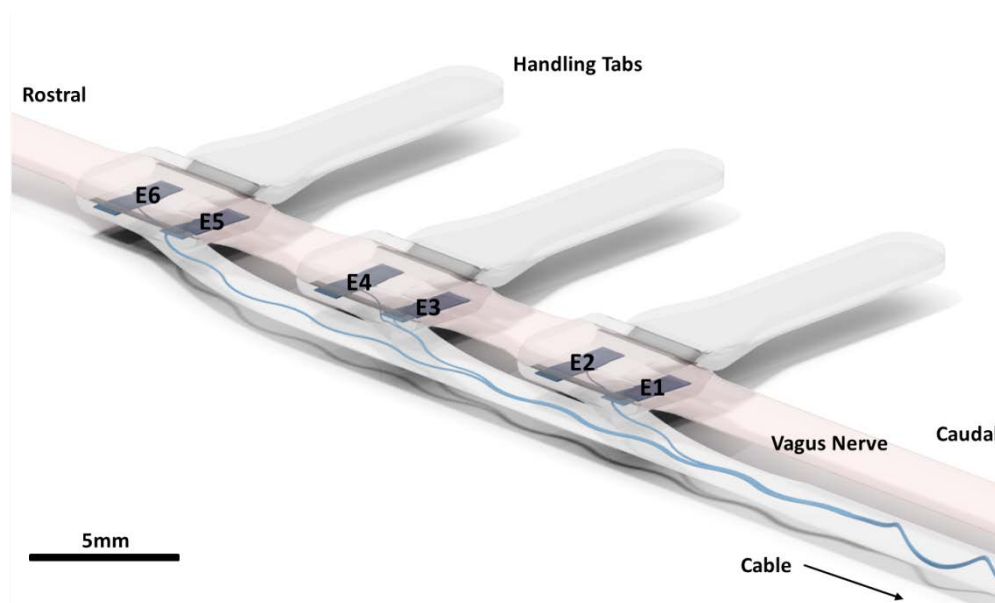
125 *Animals and housing*

126 This study was performed using five Merino ewes. All procedures were conducted with
127 approval from the animal ethics committee of the Florey Institute of Neuroscience and
128 Mental Health (No. 16-073) under the guidelines provided by the Australian Code of
129 Practice for the Care and Use of Animals for scientific purposes. All procedures were
130 also approved by the United States Army Medical Research and Materiel Command
131 Animal Care and Use Review Office (approval SSC-7486). Animals were housed
132 individually in metabolic cages (n=4) or in a larger free-ranging pen (n=1; 4 m x 4 m).
133 Sheep were provided with 800 g of oaten chaff and given 2L of water per day. The
134 intrarectal temperature was measured for up to 1 week prior to surgery (to establish a
135 baseline), and daily following surgery. Temperature of the room was kept between 20 -
136 24 °C and the light-dark cycle depended on natural day-night light.

137

138 *Design of the vagus nerve electrode array*

139 The electrode array was designed to facilitate ease of surgical application,
140 conformability to the target nerve, chronic stability and quality of neural recording. The
141 cuff array featured three bipolar platinum (Pt, 99.95%) electrode pairs embedded in a
142 medical grade silicone elastomer carrier (**Figure 1**). Bipolar pairs were used to
143 stimulate or record neural activity. Each Pt electrode had an exposed surface area of 1.5
144 mm² (2.5 x 0.6 mm). Each bipolar pair was separated by 2 mm (edge-to-edge), adjacent
145 electrode pairs were separated by 10 mm, and the distance between E1-E2 and E5-E6
146 was 20 mm. This allowed the recording of both slow and fast conducting electrically-
147 evoked compound action potential (ECAP) responses without significant masking of the
148 response by the electrical artefact (see below). The cuff was sized and shaped to slightly
149 deform the nerve, thereby ensuring good contact between the electrode and nerve
150 whilst maintaining blood flow and nerve health [20] (**Figure 1**). An elongated silicone
151 tab extending on each half of the cuff, proving easy surgical handling when positioning
152 the array around the nerve. The electrodes were connected to a cable that transitioned
153 to a percutaneous connector providing electrical connection to a portable battery
154 powered stimulator.



155

156 **Figure 1.** Schematic of the multi-cuff electrode array and cable. The array contained 6
157 Pt electrodes each with a surface area of 1.5 mm². Electrode pair E1-E2 was used to
158 chronically stimulate the nerve. All electrode pairs were able to stimulate and record
159 electrically-evoked compound action potentials from the vagus nerve. Electrode pair
160 E3-E4 (10 mm from the stimulating electrodes E1-E2) were used to record slow
161 conducting ECAPs, while electrode pair E5-E6 (20 mm from the stimulating electrodes
162 E1-E2) were used to record fast conducting ECAPs.

163

164 *Surgical implantation of the vagus nerve array*

165 Animals were anaesthetised (Time, T = week 0; sodium thiopentone: 15 mg/kg,
166 intravenous) and intubated with an endotracheal tube (cuff size 10). Anaesthesia was
167 maintained (isoflurane 2-2.5%), fractional inspired oxygen altered to maintain partial
168 oxygen (PaO₂) pressure at 100 mmHg, and ventilation regulated to maintain PaCO₂ at
169 40 mmHg [26]. Analgesia was given (Flunixin 1 mg/kg intramuscular) immediately
170 before surgery, and 4 hours and 24 hours after surgery. Intramuscular antibiotics (900
171 mg, procaine penicillin) were given before surgery and for 2 days post-operatively. The
172 vagus nerve in the lower thorax was selected as the implantation site because of the
173 difficulty in surgically accessing the abdominal vagus in the sheep. Using sterile surgical
174 techniques, the skin and muscle of the left side of the animal was incised at the region of
175 the 6th rib and a thoracotomy performed. Following removal of the 6th rib, the lungs
176 were gently retracted to allow access to the anterior (left) vagus nerve of the lower
177 thorax. The vagus nerve was carefully dissected away from the oesophagus and
178 surrounding fat, and the three pairs of cuff electrodes were placed and secured around
179 the nerve. The array was mechanically stabilised by suturing the cable to superficial
180 connective tissue on the oesophagus. The cable traversed intercostal muscles to exit
181 between the 5th and 7th rib and was tunnelled subcutaneously to the exit location on the
182 dorsal region of the thorax. Overlying muscle and skin layers were sutured closed and

183 the animals were allowed to recover. Implantation of the vagus nerve array (from induction
184 of anesthesia to the final suturing procedure) in typically took 90 – 120 minutes.

185

186 *Stimulator design and chronic stimulation program*

187 One month following the implantation of the electrode array, four of the five animals
188 commenced a chronic stimulation program using a custom built programmable back
189 pack stimulator [27]. Charge balanced biphasic current pulses of 0.4 $\mu\text{C}/\text{phase}$ were
190 continuously delivered generating a charge density of 27 $\mu\text{C}/\text{cm}^2/\text{phase}$. The stimulus
191 was delivered at 30 pulses per second (pps) using a duty cycle similar to that used in a
192 recent clinical VNS trial (30 s ON, 150 s OFF, Table 1) [12]. Charge recovery was
193 achieved *via* electrode shorting between stimulus pulses [28]. The animal's behavioural
194 responses to the stimulation were monitored carefully.

195

196 *Electrode impedance and electrically-evoked compound action potentials*

197 Electrodes were monitored daily by measuring their common-ground impedance. The
198 peak electrode voltage developed at the end of the first phase of a 200 μs pulse (0.65
199 mA current) was measured and the impedance calculated using Ohm's law [29]. ECAPs
200 were recorded weekly in order to monitor neural function. Biphasic current pulses (10
201 pps, 200 μs per phase, 50 μs interphase gap) were used to stimulate electrodes E1-E2.
202 Neural responses were recorded from bipolar electrodes 10 mm (E3-E4) and 20 mm
203 (E5-E6) from the site of stimulation. Two sets of recordings were made at currents from
204 below threshold to 2.0 mA in 0.1 mA steps. Recordings were sampled at a rate of 100
205 kHz, filtered (high pass: 200 Hz; low pass: 2000 Hz), amplified ($\times 10^3$) and 50
206 presentations were averaged for each response. The ECAP threshold was defined as the
207 minimum stimulus intensity producing a response amplitude of at least 1 μV in both
208 recordings within a latency window of 4-8 ms following the stimulus.

209

210 *Monitoring off-target effects to stimulation*

211 Food intake and faecal output were measured at the same time each day to assess off-
212 target effects of the stimulation on gut motility. These measurements commenced one
213 week prior to implantation surgery and continued until the day of termination. The
214 median value for each week was analysed. Respiration patterns were recorded in
215 conscious, freely moving sheep by placing a piezo-electric respiration band (UFI model
216 1132 Pneumotrace II) around the abdomen. Care was taken to place the sensor over the
217 point of largest excursion during respiration. Animals were habituated to the
218 respiration band for at least 1 day before continuous baseline recordings were made
219 with the experimenter out of the room. Respiration rate was then measured within 4
220 days following the onset of chronic stimulation (n=3 sheep;) and again after 4 – 8 weeks
221 of continuous stimulation (n=4 sheep;). Electrocardiograms (ECGs) were
222 simultaneously recorded to measure heart rate using two vagus nerve electrode pairs. A

223 breathing and heart rate trial consisted of: 30 seconds OFF (a non-stimulation baseline),
224 30 seconds 'ON' (2 mA, 200 μ s, 30 pps) and 30 seconds OFF (recovery). Trials were
225 repeated up to 21 times in one session. On the day of termination, stimulus induced
226 changes to heart rate were also assessed while the animal was anaesthetised by
227 recording the potential differences between three subcutaneous needle electrodes
228 placed in the fore and hind limbs.

229

230 ECGs were recorded over a two minute period without stimulation followed by two
231 minutes of continual stimulation (2 mA, 200 μ s, 30 pps), and then a second two minute
232 period of stimulation. This procedure was repeated at 10 and 2 pps. The ECG signal was
233 amplified using a WPI Iso-80 bioamp (Gain: $\times 10^3$; high pass: 5Hz; low pass 10kHz) and
234 all signals digitized using a CED Micro3 1401 A/D interface and Spike 2 software. Heart
235 rate was calculated from the ECG waveform using a spike detection algorithm in the
236 Spike2 software.

237

238 *Histological processing and analysis*

239 On completion of the experimental period, animals were euthanized with sodium
240 pentobarbitone (100 mg/kg, I.V). The anterior vagus nerve of the lower thorax together
241 with the entire implanted electrode array (E1-E6) was exposed and images of the array
242 in situ were generated and macroscopic observations made. Next, the array with the
243 nerve and surrounding tissue in place was rapidly removed from the carcass and fixed
244 in 4% paraformaldehyde in 0.1 M phosphate buffer (pH 7.3) for 48 hours at 4°C. On
245 completion of the fixation, tissue was thoroughly washed (3 x 20 minutes in phosphate
246 buffered saline). Electrode pair E3 - E4 and the implanted vagus nerve were removed
247 whole and processed separately for assessment of the electrode-neural interface (see
248 Methods section: Electrode neural interface processing). Tissue taken 20 mm rostral
249 and caudal from the electrode array was taken as an intra-animal control. Electrode
250 pairs E1 - E2 and E5 - E6 were carefully dissected from the nerve and the region of the
251 nerve adjacent to the electrodes were labelled using tissue dye (Davidson's Marking
252 system, Bradley Products) [30]. Neural tissue was processed for paraffin wax
253 embedding, sectioned (5 μ m), representative sections stained with hematoxylin and
254 eosin (H&E) and mounted with DPX. Electrodes were cleaned (sonication in pyroneg
255 solution and rinsed in water), and examined for evidence of Pt corrosion using a
256 scanning electron microscope (sem, see below). The anterior vagus nerve adjacent to
257 the stimulated electrodes (E1, E2) and unstimulated electrodes (E5, E6) was examined
258 as were regions of nerve just caudal and rostral to the electrode array. Total fascicle
259 area at these locations were quantified and compared statistically. Light microscope
260 images of the nerve sections were taken (Zeiss Axioplan microscope), and these data
261 analysed using Image J.

262

263 *Clinical pathology examination:*

264 Histological sections of the vagus nerve from all implanted animals (n=5) and a non-
265 implanted control nerve were examined by a clinical pathologist for evidence of neural

266 damage, the extent and nature of the inflammatory response and any evidence of
267 infection. The examination was performed using appropriate blinded techniques.

268

269 *Scanning electron microscopy imaging and analysis*

270 Following dissection, both stimulated (E1, E2) and unstimulated (E5, E6) electrode
271 pairs from each animal were examined for evidence of Pt corrosion (FEI QUANTA 200
272 sem).

273 Each electrode was examined over a range of magnifications (x 600 – x10,000). The
274 surface condition of each Pt electrode was evaluated by an investigator blinded to the
275 experimental groups. Surface features, including mechanical damage, pitting corrosion,
276 intergranular corrosion and surface deposits, were recorded. The severity of Pt
277 corrosion was graded from 0 (no corrosion); 1 (no evidence of corrosion but electrode
278 at least partially coated with organic material); 2 (localized minor corrosion); 3
279 (localized moderate corrosion); 4 (widespread corrosion); 5 (severe and extensive
280 corrosion) [31].

281

282 *Electrode neural interface processing*

283 Electrode pair E3 and E4 and the underlying vagus nerve were collected for processing
284 to enable visualisation of the electrode-neural interface. The specimens were
285 dehydrated in ethanol and immersed in degassed epoxy resin. After embedding, the
286 specimens were sectioned using a grinding technique [32]. Every 300 µm the surface
287 was polished, stained with toluidine blue and photographed under a light microscope.
288 These digital images provided records of the position of the anterior vagus nerve
289 relative to the Pt electrode.

290

291 *Statistical analysis*

292 Differences in evoked neural thresholds, food intake, faecal output and heart rate data
293 over time were examined statistically using an ordinary or repeated measures (RM)
294 one-way analysis of variance and appropriate *post-hoc* comparisons. Differences
295 between commonground impedance of stimulated and unstimulated electrodes over
296 time was assessed using a two-way ANOVA. Statistical differences in histological
297 measurements between implanted and non-implanted tissue was assessed using a one-
298 way ANOVA or paired two-tailed T-Test). Statistical comparison of Pt electrode surfaces
299 was determined using a Mann-Whitney rank sum test (stimulated and control
300 electrodes). Significance was accepted if $P \leq 0.05$.

301

302 **3. Results**

303 *Implantation period*

304 The mean \pm standard error of the mean (S.E.M) vagus nerve array implantation period
305 for all sheep (n = 5) was 11.9 ± 1.0 weeks. Four sheep were successfully implanted for
306 >12 weeks, all of which were electrically stimulated, while one animal (VNc5), randomly
307 selected as an unstimulated control, was sacrificed at 7.9 weeks post implantation due
308 to complications not related to the implantation of the vagus nerve array (**Table 1**).

309

310 **Table 1.** Summary of sheep and stimulation used in the safety cohort.

Sheep	Implantation duration (weeks)	Stimulated electrodes	Charge per phase (nC)	Total switch on time (hours)	Adverse events	Electrode region at autopsy
VNS1	12.8	E1-E2	400	984	None	Benign tissue fibrosis; no infection
VNS2	13.6	E1-E2	400	1524	None	Benign tissue fibrosis; no infection
VNS3	13.1	E1-E2	400	1800	None	Benign tissue fibrosis; no infection
VNS4	12.1	E1-E2	400	1404	None	Benign tissue fibrosis; no infection
VN _c 5	7.9	N/A	N/A	N/A	Yes - event not related to device	Less mature tissue fibrosis; no infection

311 N/A, not applicable.

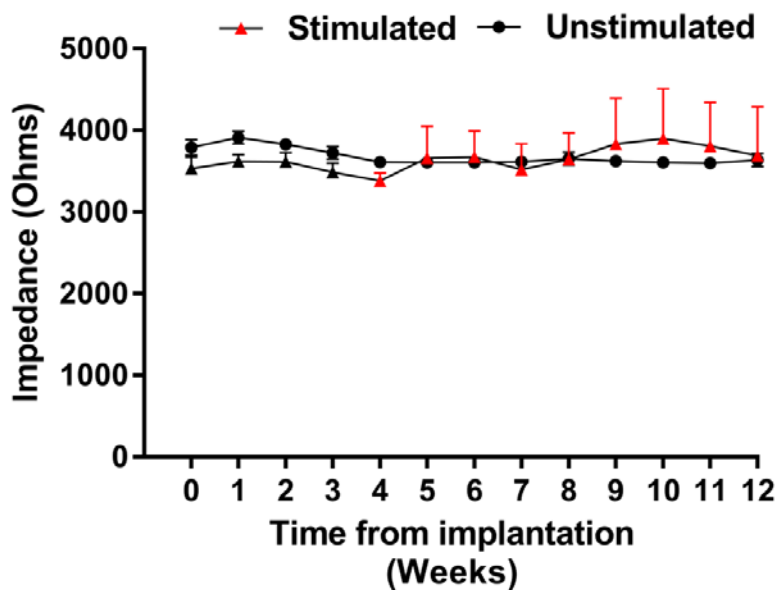
312

313 *Post-surgical monitoring*

314 During the implantation period, the rectal temperature of sheep ranged from 39.0 to
315 39.8 °C, which is considered normal. Surgical incision sites healed quickly and remained
316 free from infection. The skin in proximity with the percutaneous connector and
317 subcutaneous cable remained free from infection and irritation. Furthermore, no
318 adverse responses (e.g. coughing, agitation or dyspnea) were observed during the
319 chronic stimulation program.

320 *Electrode impedance during implantation*

321 All electrodes from each animal in this study remained functional throughout the
322 implantation/stimulation period (n = 30 electrodes; n = 5 sheep; **Figure 2**). There was
323 no significant difference between the impedance of chronically stimulated and
324 unstimulated electrodes over the implantation period ($P = 0.37$, RM two-way ANOVA,
325 time x stimulation; **Figure 2**).



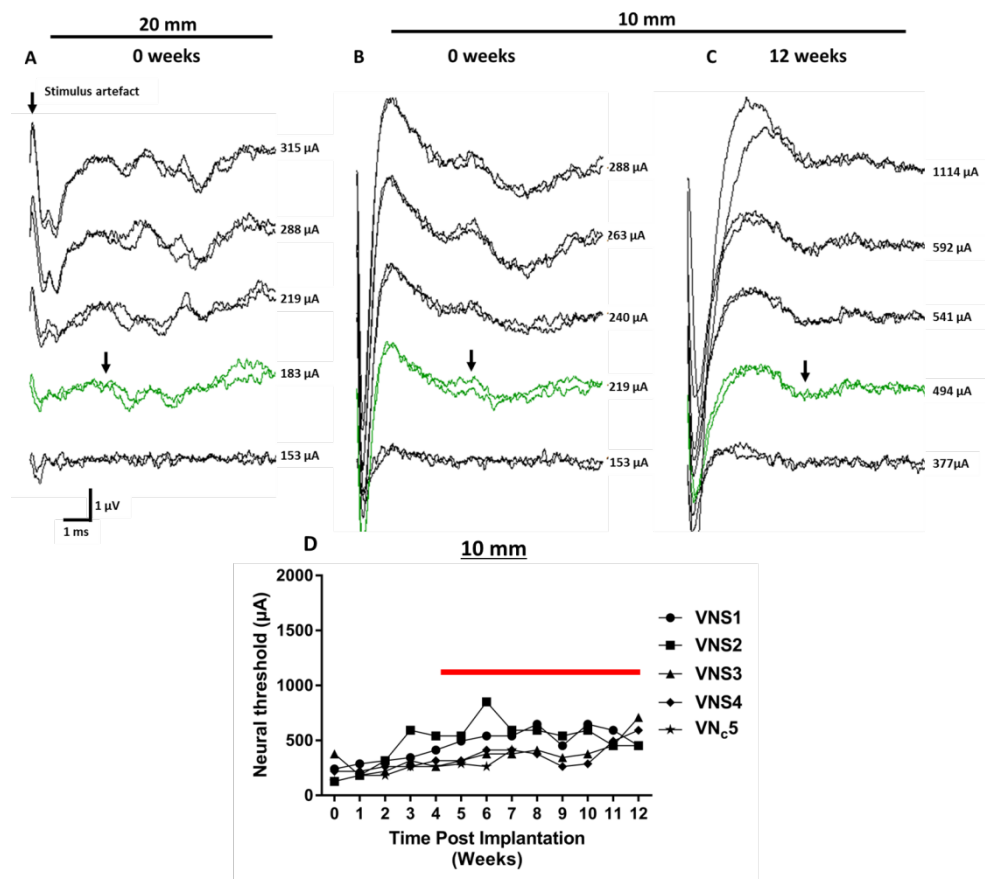
326

327 **Figure 2.** Electrode impedance recorded weekly during the implantation period for all
328 electrodes in this study. All electrodes (n = 30) remained functional during this period,
329 and there were no significant differences between impedance of stimulated (red; n=8)
330 and unstimulated (black; n=22) electrodes ($P = 0.37$). Data show mean common-ground
331 impedance +S.E.M. While all error bars have been plotted, some are obscured by the
332 symbols.

333

334 *Electrically-evoked neural responses*

335 ECAPs were successfully recorded from all implanted animals (n=5) over the duration
336 of the implantation period. Representative ECAP waveforms recorded at 20 mm from
337 the stimulation site are shown in **Figure 3A** (indicated by arrow) while the recruitment
338 of slower neural populations, recorded at 10 mm from the stimulation site, is displayed
339 in **Figures 3B-C** (indicated by arrow). Although there was a trend for an increase in
340 ECAP threshold over the implantation period, this difference was not statistically
341 significant (n = 4; $P = 0.08$; RM one-way ANOVA; **Figure 3D**). The average latency of the
342 ECAP recorded 10 mm from the stimulation site was 7.0 ± 1.2 ms (T = 0; estimated
343 conduction of 1.4 ± 0.2 m/s; **Figure 3B-C**) did not change during the implantation period
344 ($P = 0.49$, n = 4). Furthermore, neural thresholds remained well below the stimulus
345 levels used for chronic stimulation (2 mA, 200 μ s pulse width), thereby confirming that
346 the vagus nerve was stimulated at suprathreshold levels for the duration of the stimulus
347 program.



348

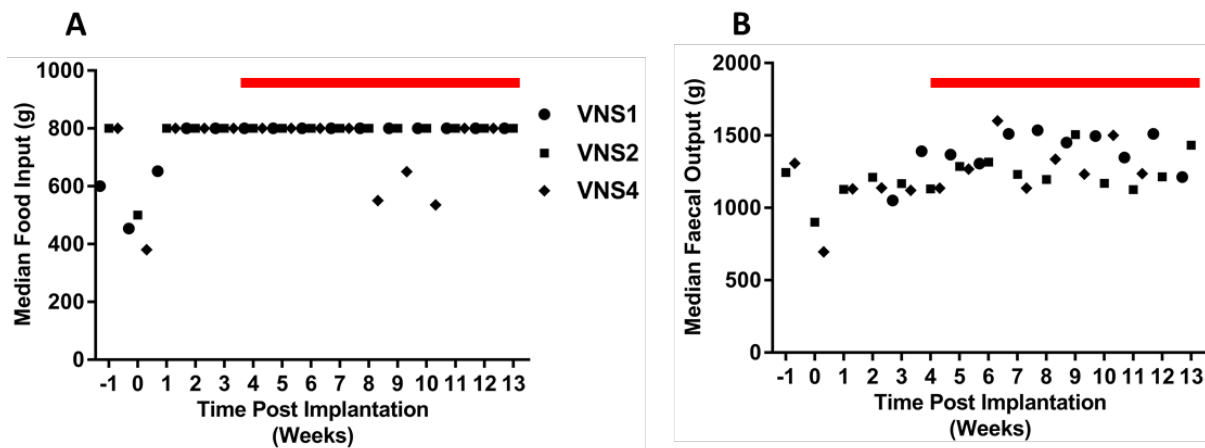
349 **Figure 3.** Electrophysiological recordings of the vagus nerve during the
350 implantation period. **A:** ECAPs (indicated by arrow) of faster conduction
351 fibers were detected using recording electrodes 20 mm from the stimulating
352 electrodes pairs at 0 weeks (latency: 4.4 ms, conduction: 4.5 m/s). **B-C:**
353 ECAPs of slower conduction fibers were recorded at a site 10 mm from stimulating
354 electrodes at 0 weeks (**B**, latency: 4.1 ms, conduction: 1.4 m/s) and 12 weeks
355 (**C**, latency: 5.0 ms, conduction: 2 m/s) from the same animal (VNS4). **D:**
356 Quantification of neural response thresholds (indicated by the green
357 recordings in A-C) from 10 mm electrode configuration (T = 0) show no
358 changes ($P = 0.08$) in thresholds over the implantation period. The red bar
359 indicates the stimulation period). In **A-C**, the arrows indicate the times of the
360 ECAP peak at the recording electrode.

361

362 *Off-target effects pre- and post- the onset of stimulation*

363 The sheep that were stimulated did not display any adverse behaviour indicative of
364 pain, alarm or discomfort at either the initial onset of stimulation or for the duration of
365 the stimulation program. Food intake and faecal output (per day, **Figure 4A, B**) was
366 analysed (RM one-way ANOVA, Dunnett's *post hoc* test using T = -1 as control) for
367 stimulated animals maintained in metabolic cages (VNS1, 2, 4). Food intake remained
368 similar to baseline following implantation surgery (T = 0 to 12 weeks; n = 3; $P = 0.12$;
369 **Figure 4A**). Daily faecal output was reduced during the first week after surgery (T = 0; P
370 = 0.02) compared with pre-surgical baseline values. However, between 1 and 12 weeks

371 faecal output remained similar to pre-surgical baseline values ($P = 0.25$; $n = 3$; **Figure**
372 **4B**).



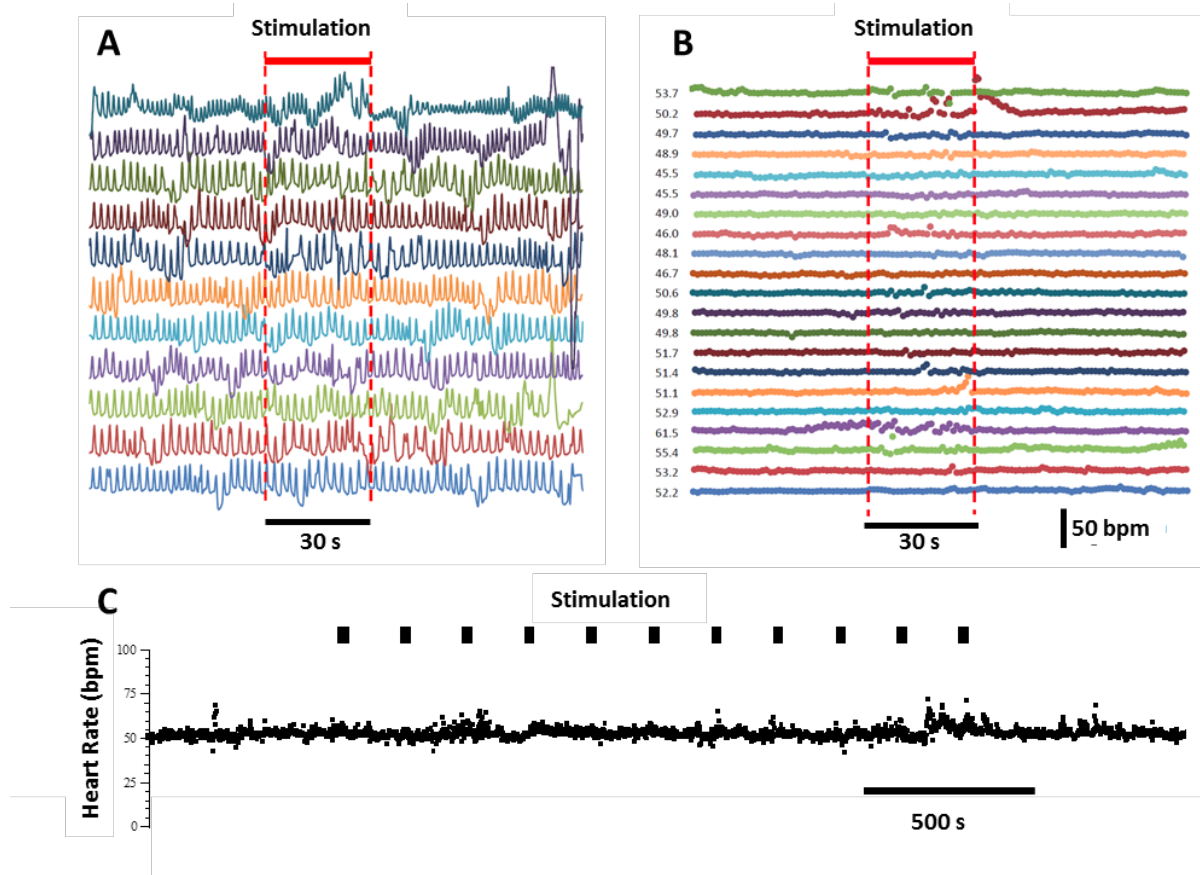
373 **Figure 4.** Effect of stimulation on food intake and faecal output. **A:** Food intake
374 (maximum 800 g) per day remained similar to pre-surgery levels ($T=-1$) following
375 implantation surgery and during the chronic stimulation (indicated by red bar) ($T=0$ to
376 12 weeks, $P = 0.12$). **B:** Although faecal output (per day) decreased during the first week
377 post-surgery ($T=0$, $P = 0.02$), no change was seen from baseline ($T=-1$, $P = 0.25$) in
378 subsequent weeks.

379
380
381

382 During the period in which the vagus nerve was being stimulated, we assessed
383 respiration and heart rate in awake, freely moving sheep within 4 days of first switching
384 on the chronic stimulation ($n = 3$ sheep) and after 4 weeks of continuous stimulation (n
385 $= 4$ sheep). Respiration varies greatly over time in conscious sheep. We inspected the
386 recordings for any abrupt change in respiration pattern that coincided with the start of
387 the stimulus period over multiple stimulus trials. Within 4 days of the onset of the
388 chronic stimulation program there were no observed changes to respiration rate in one
389 animal, while two animals exhibited a transient slowing of respiration that coincided
390 with the onset of stimulation in 15/21 and 8/12 trials respectively. A stimulus induced
391 reduction in respiration rate became less evident during the course of the chronic
392 stimulation program. At 4 weeks of stimulation, two animals showed no stimulus
393 induced effects on respiration (**Figure 5A**) and the third animal exhibited only small
394 changes in respiration during the onset of stimulation (observed in 6/11 trials).

395 Heart rate was also measured in awake, freely moving sheep. Heart rate data from
396 multiple stimulation trials before, during and after each 30 s stimulation period was
397 analysed in each sheep separately using a RM one-way ANOVA. When tested within 4
398 days of the onset of stimulation, there was no significant effect of stimulation on heart
399 rate in three sheep ($P \geq 0.05$) and only a small increase in one animal (VNS3; 73 to 78
400 beats per minute; $P = 0.01$). This effect was not seen in any of the four stimulated sheep
401 tested at a later time point ($P \geq 0.05$; **Figure 5B**). At the time of termination, changes in
402 heart rate under anaesthesia before, during and after each 30 s stimulation period was

403 measured. Under these conditions, there were no stimulus induced changes in heart
404 rate in any tested animal (n=4).



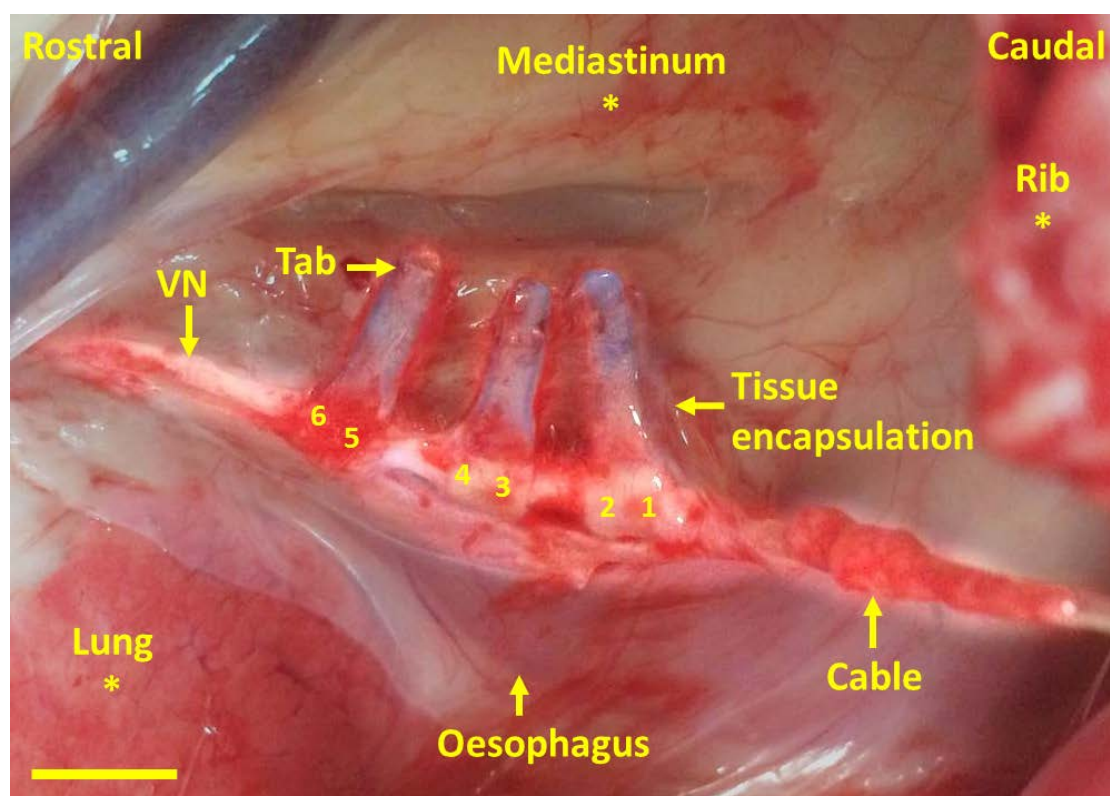
405
406 **Figure 5.** Assessment of potential off-target effects in response to anterior vagus nerve
407 stimulation. **A:** Representative respiration traces (VNS4) recorded at 4 weeks following
408 onset of chronic stimulation illustrating the baseline variation in the recordings; there
409 was no evidence of a stimulus induced change in respiration. **B:** A trace from one sheep
410 (VNS4) is an example of the heart rate recording trials (n = 21) taken within the first 4
411 days of the onset of stimulation. No consistent changes to heart rate were observed
412 within the 30 s stimulation period. Mean heart rate for each recording is also illustrated
413 to the left of each recording trial. **C:** Longitudinal recording of heart rate in one sheep
414 (VNS4) recorded at 4 weeks following onset of stimulation. Again, no changes to heart
415 rate were consistently observed within the 30 s stimulation period.

416

417 *Autopsy observations of array in vivo*

418 On the day of euthanasia, macroscopic examination of the status of the tissue
419 surrounding the percutaneous connector, cable and vagus nerve electrode array was
420 undertaken (Table 1). In all implanted animals (n = 5), fibrous tissue surrounding the
421 percutaneous connector and the subcutaneous cable was free from infection and no
422 signs of irritation or inflammation were observed macroscopically. The cable
423 transitioning point through the intercostal muscle layer into the thoracic cavity was free

424 from infection and had healed well. There was minimal scar tissue, and the intercostal
425 muscle tissue around the cable was unencumbered. Examination of the multi-cuff array
426 *in vivo* showed that a thin fibrous tissue encapsulation had formed around the array
427 (**Figure 6**), and there was no distortion (i.e. twisting) of the vagus nerve. The tissue
428 encapsulation was restricted to the vicinity of the array and cable, and did not spread
429 from this area and affect adjacent tissues (**Figure 6**). Attachment of the electrode array
430 had not caused any macroscopic damage to the nerve, and blood vessels were typically
431 observed running longitudinally along the implanted vagus nerve. No irritation,
432 haemorrhaging or haematomas were observed within adjacent tissue (oesophagus, lung
433 and mediastinum).
434



435
436 **Figure 6.** *In vivo* macroscopic observation of the implanted array. Autopsy image shows
437 the typical gross tissue response around the electrode array following 12 weeks of
438 implantation (VNS1), and illustrates the anterior vagus nerve of the lower thorax (VN)
439 and the electrode array (with each of the six electrodes identified numerically), the
440 three handling tabs and the cable. Scale bar = 10 mm.

441
442

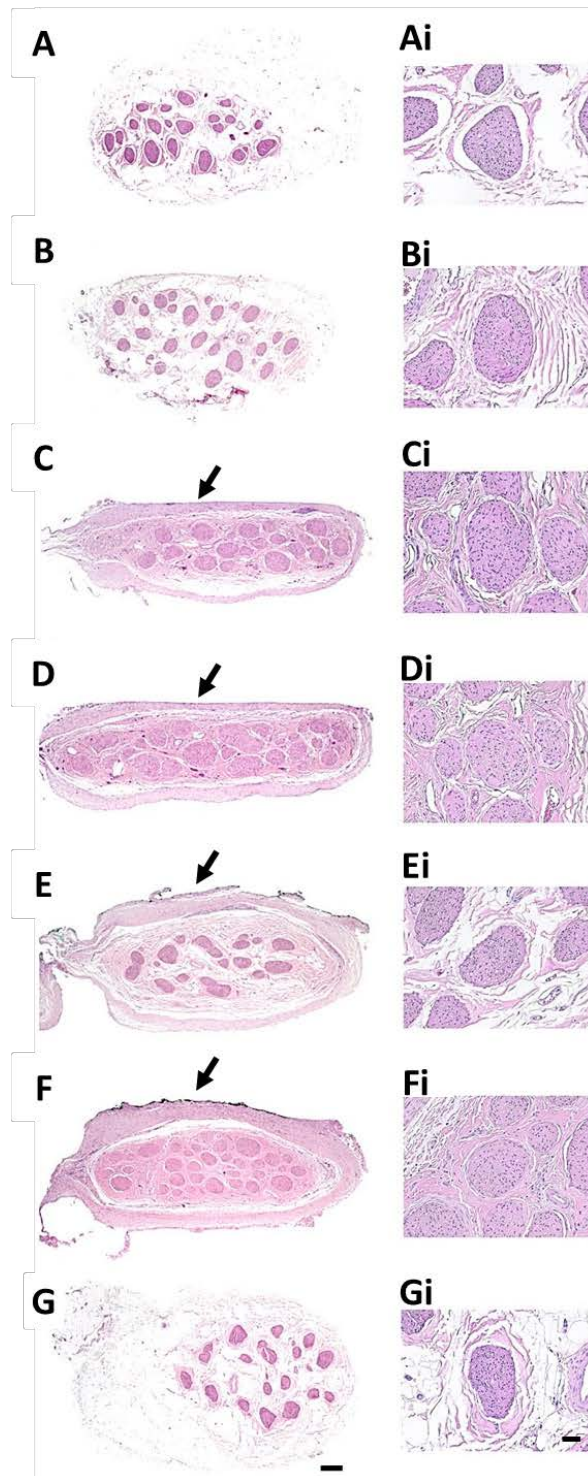
443 *No histological damage seen in implanted vagus nerves*

444 Representative micrographs of the tissue response of the vagus nerve following chronic
445 implantation and electrical stimulation are illustrated in **Figure 7**. The vagus nerve
446 from a non-implanted control animal is included in this figure for comparison (**Figure**
447 **7A**).

448 A clinical pathologist (author: RAW) reported no damage to nerve fascicles due to the
449 implant and/or electrical stimulation, and no evidence of granulation tissue or the
450 infiltration of acute inflammatory cells (**Figure 7C-F**). There was a mature, but benign,
451 fibrous tissue response around the epineurium that was not observed to have chronic
452 inflammatory cells within it. There was no observed histological difference between
453 stimulated (E1 and E2) and unstimulated (E5 and E6) regions of the nerve. However, a
454 foreign body and histiocytic response around the periphery of the tissue capsule had
455 developed along the boundary of the nerve with the cuff electrode array in both
456 stimulated and unstimulated tissue (**Figure 7C-F**, indicated by arrows). The
457 distribution and appearance of blood vessels within the fascicles appeared normal in
458 both stimulated and unstimulated tissue. The fascicle shape was distorted transversely
459 due to the design of the cuff electrode, similar to that described previously [20]. In a few
460 sections, there was evidence of small regions of chronic inflammation inside the fibrotic
461 tissue capsule. These inflammatory pockets rarely encroached into the boundary of the
462 epineurium, and mostly remained within the confines of the fibrotic tissue
463 encapsulation.

464 Tissue taken rostral (**Figure 7B**) and caudal (**Figure 7G**) to the implanted electrode
465 array did not have a fibrous tissue response around the epineurium. Typically, these
466 rostral and caudal sites had less or no fibrous tissue present between fascicles, when
467 compared with implanted regions of nerve (**Figure 7C-F**). The tissue response in
468 control animal VN_c5 (implanted for 2 months) was less mature than the response in the
469 animals implanted for 3 months (VNS1-4) as evidenced by the greater number of
470 fibroblasts in the histology of VN_c5 (data not shown). Small deposits of hemosiderin
471 were occasionally observed in some sections of the implanted tissue, implying that
472 some localized bleeding had occurred at the time of surgery.

473 Fascicle quantification was conducted by measuring both fascicle area and the total
474 cross-sectional area of the nerve from histological sections taken from tissue 20 mm
475 rostral and caudal to the implant, adjacent to stimulated electrodes (E1 and E2) and
476 adjacent to unstimulated electrodes (E5 and E6). The control animal (VN_c5) was not
477 included in analysis as it had been implanted for 7 rather than 12 weeks. There was no
478 significant difference in the total fascicle area between these sites ($P = 0.64$; one-way
479 ANOVA) indicating that neither chronic implantation nor stimulation resulted in neural
480 loss, compared with regions of the nerve proximal (rostral) or distal (caudal) to the
481 electrode array. The proportion of total fascicle area compared with the total cross
482 sectional nerve area (i.e. the fascicle packing density) was assessed between stimulated
483 (E1 and E2) and unstimulated (E5 and E6) tissue and showed no statistically significant
484 difference ($n=4$; paired two-tailed T-Test; $P = 0.86$). This fascicle packing density data
485 from tissue adjacent to E1, E2, E5, E6 was therefore combined. There was a significant
486 increase in the fascicle packing density between implanted tissue ($23.9 \pm 1.2\%$) versus
487 the two non-implanted regions of the vagus nerve ($17.0 \pm 2.5\%$; two-tailed paired T-
488 test; $P = 0.001$; **Figure 7B, G**).



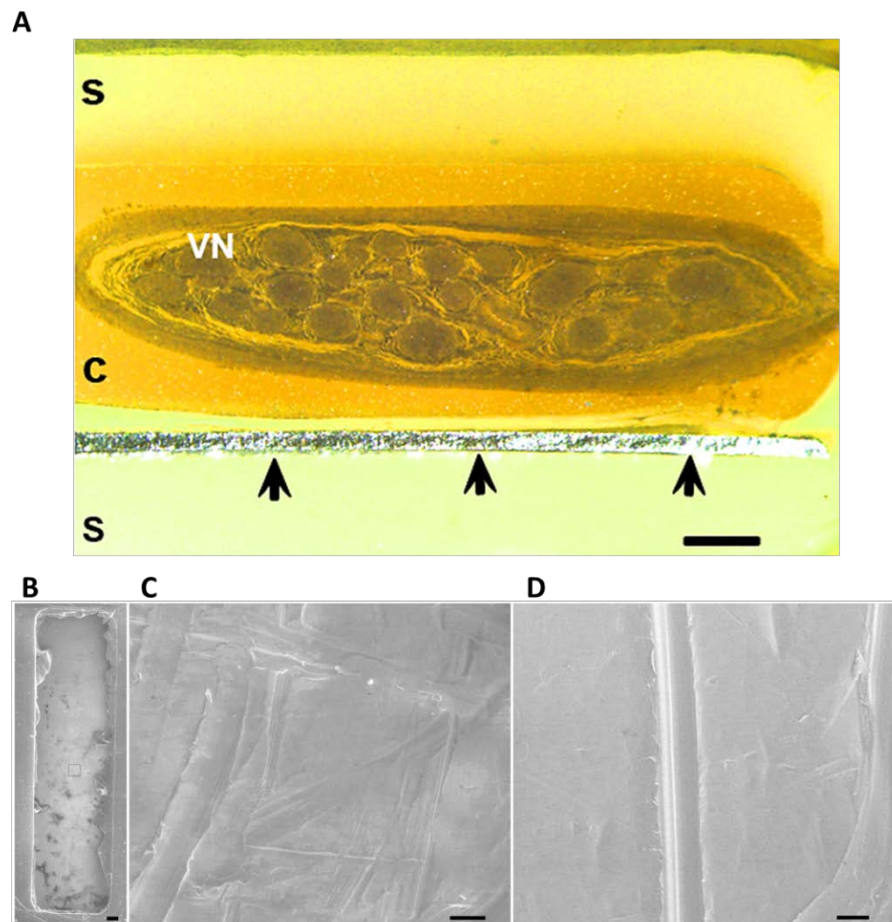
491 **Figure 7.** Histopathology of the chronically implanted anterior vagus nerve. **A-G:**
492 Sections of vagus nerve tissue were sectioned and stained with haematoxylin and eosin
493 (H&E) for histopathological assessment by a blinded observer. Images show non-
494 implanted nerve (**A**), and tissue taken 20 mm rostral (**B**, VNS4) and caudal (**G**, VNS3) to
495 the electrode array. Tissue adjacent to electrodes E6 (**C**, VN_c5), E5 (**D**, VN_c5), E2 (**E**,
496 VNS3) and E1 (**F**, VNS1) were assessed for damage and signs of inflammation. The
497 tissue in contact with the Pt electrode (**C-F**) is indicated by arrows. Higher power

498 images of each section are illustrated in **Ai-Gi**. Scale bar for images **A-G**: 200 μm ; **Ai-Gi**:
499 50 μm .

500

501 *Electrode neural interface examination*

502 By embedding and sectioning electrodes E3 and E4 together with the vagus nerve
503 contained within these electrodes, we were able to examine the electrode neural
504 interface in some detail. As illustrated in **Figure 8A**, the vagus nerve and its fibrous
505 tissue capsule can be identified within the cavity (C) formed around the nerve by the
506 cuff electrode. In all animals examined ($n = 5$), the nerve and its associated tissue
507 capsule did not always occupy the entire cavity. While we cannot dismiss the possibility
508 of tissue shrinkage, these results indicate that the nerve may not form a tight interface
509 with the electrodes. However, the cross-sectional profile of the nerve reflects the
510 longitudinal distortion observed in the histological sections (**Figure 7C-F**). Inspection
511 of the region of the cavity in each animal showed no evidence of tissue adhesions,
512 cellular debris or an accumulation of inflammatory cells. As illustrated in **Figure 8A**,
513 the Pt electrode (indicated by arrows) is evident at the interface between the silicone
514 carrier (S) and the cavity. The vagus nerve is positioned $\sim 100\text{-}200\ \mu\text{m}$ from the
515 electrode and this was typical for all animals examined using this technique.



516

517 **Figure 8.** Assessment of electrode–neural interface and Pt electrode surface. **A:**
518 Representative image of epoxy resin embedded electrode array (unstimulated, E3,
519 VN_c5), silicone cuffs (S), nerve cavity (C) and implanted vagus nerve (VN). Arrows
520 indicate the Pt electrode surface. **B-C:** Low (B) and high (C) magnification micrographs
521 of an electrode used for chronic stimulation (E2; VNS1). Despite score marks associated
522 with manufacturing, there was no sign of corrosion. **D:** High magnification micrograph
523 from an electrode not used for chronic stimulation (E5, VNS2), again illustrated
524 manufacturing score marks without evidence of corrosion. Scale bar for **A:** 200 µm; **B:**
525 100 µm; **C-D:** 10 µm.

526

527 *No corrosion seen in chronically stimulated electrodes*

528 **Figure 8** illustrates the typical surface features associated with a chronically stimulated
529 (**Figure 8C**) and an un-stimulated recording electrode (**Figure 8D**). Typical surface
530 features included manufacturing marks; however there was no evidence of Pt corrosion
531 observed on any electrode in the present study. Stimulated electrodes did show
532 significantly more protein and fibrous tissue on the electrode surface compared with
533 the unstimulated electrodes ($P < 0.002$; Mann-Whitney rank sum test).

534

535 **4. Discussion**

536 The present study evaluated the long-term safety of a novel multi-cuff peripheral nerve
537 electrode array in a pre-clinical ovine model, and trialled a new target location on the
538 anterior vagus nerve in the lower thorax, below the branches to the larynx, heart and
539 lungs in order to reduce off-target effects during stimulation. The results show that
540 chronic implantation and stimulation of this peripheral nerve array is safe and provides
541 an effective means of monitoring electrically-evoked vagus nerve activity. The multi-cuff
542 array remained functional during the implantation period and the electrode properties
543 were unaffected by chronic electrical stimulation. Following implantation of the array,
544 the vagus nerve showed no change in ECAP threshold over time, and no adverse
545 inflammatory response or neural loss was seen in the histology. There were no
546 measurable changes to eating, defecation and few sustained changes to heart rate during
547 stimulation. While respiratory rate exhibited small changes at the onset of stimulation
548 in three animals, they diminished with implant duration. Taken together, these findings
549 support the use of this novel peripheral nerve array for VNS at a site located below the
550 branches to the larynx, heart and lungs, as a treatment of IBD.

551

552 *Device design evaluation*

553 The cuff array developed in the present study was manufactured using biocompatible
554 materials (platinum and medical grade silicone), which have long histories of successful

555 application in medical devices [33]. The cuff design aimed to reshape the nerve slightly
556 for optimal contact onto the active Pt electrode surface. This design is known as the flat-
557 interface nerve electrode (FINE) and has been used extensively by Durand and
558 colleagues to improve recording of somatic (peripheral) nerves in animal and
559 intraoperative human studies [20, 34-36]. Furthermore, FINE electrode arrays have
560 been successfully implanted onto the peripheral nerves of amputees for over a year, in
561 order to evoke touch sensations via electrical stimulation [37]. The electrode array used
562 in the present study was safely implanted chronically onto the peripheral nerve of a
563 large animal model, and all electrodes remained functional and impedances stable over
564 the implantation period. There was more variability in the impedance of the stimulated
565 electrodes between 5 – 12 weeks due to one electrode exhibiting a rise in impedance
566 (**Figure 2**). However, this electrode remained functional, as indicated by the electrode's
567 ability to evoke neural responses. The absence of tissue adhesions between the nerve
568 and electrode array suggests that the cuff-array can be removed with minimal trauma to
569 the underlying nerve. The ability to safely remove an electrode array is an important
570 design consideration for the development of a safe device for clinical application [21].

571
572 A feature of the present electrode array was the ability to record multiple neural
573 populations. The electrode array has two recording sites, 10 mm and 20 mm from the
574 stimulating electrode pair. A subpopulation of thoracic vagal fibers exhibit fast
575 conduction so there is a need to have some separation (i.e. 20 mm) between the
576 stimulating and recording electrodes in order to record these responses outside the
577 latency of the stimulus artefact. In contrast, a majority of thoracic vagal fibers exhibit
578 slow conduction, are poorly synchronized and recordings are diminished with
579 increasing distance between the stimulating and recording electrodes. Therefore, using
580 a more proximal recording site (10 mm) is optimal for a slower conduction fiber type.

581
582 These electrically-evoked slow conduction fibers had an average conduction of 1.4 m/s.
583 This is in the same range as C-fiber conduction [15], suggesting that the slow
584 conduction fibers evoked by the vagus nerve array are C-fibers. Furthermore,
585 stimulation levels were supra-threshold throughout the duration of the study. This is an
586 important property of the electrode array, as it is likely that abdominal vagal C-fibers
587 are involved in driving the anti-inflammatory mechanisms of VNS [16, 17].

588 589 *Biocompatibility and physical safety of the multi-cuff array*

590 Peripheral nerves are highly vascularised and consist of fibers that transfer sensory and
591 motor information, *via* action potentials to and from the brain [38], in addition to the
592 transport of cellular components via retrograde and anterograde transport. Therefore,
593 compression from the electrode cuff may cause occlusion, disruptions to the nerve
594 physiology, disruption of axonal transport and even neural degeneration [39, 40].
595 Depending on the severity of the compression, injury-induced neural degeneration is
596 likely to be observable by 3 months [41]. In the present study, histopathological

597 assessment of the implanted vagus nerve showed no evidence of neural loss.
598 Furthermore, total fascicle area (containing vagal axon fibers) was similar to
599 rostral/caudal tissue, suggesting no significant neural degeneration had occurred as a
600 result of the chronic implantation of these cuff electrodes. Numerous blood vessels were
601 observed throughout intra- and extra-fascicular areas of the implanted tissue. In
602 addition, ECAPs were recorded throughout the implantation period, suggesting that
603 vagus nerve function was not disrupted.

604

605 *Electrical safety of stimulation parameters*

606 The stimulation parameters used in the present study (0.4 $\mu\text{C}/\text{phase}$ developing a
607 charge density of 27 $\mu\text{C}/\text{cm}^2/\text{phase}$), were well within the safety limit defined by
608 Shannon (1992) or Pt corrosion limits defined electrochemically [24, 42]. Therefore, it
609 is not surprising that no electrically-induced neural damage or Pt corrosion was seen.

610 Previous clinical studies that investigated VNS using a Cyberonics device as a therapy
611 for Crohn's disease applied continuous stimulation of 10 pps, 500 μs pulse width, 1.25
612 mA current and duty cycle of 30 s ON, 300 s OFF [12]. Here, we continually using a
613 higher rate (30 pps) and current (2 mA), while the duty cycle was nearly doubled (30 s
614 ON, 150 s OFF). A shorter pulse width (200 $\mu\text{s}/\text{phase}$) was selected to reduce the
615 duration of the electrical artefact in order to improve the quality of the ECAP
616 recordings. The SEM analysis of stimulated Pt electrodes showed no corrosion,
617 compared with unstimulated electrodes. Taken together, this result, combined with the
618 histopathological observations of the implanted vagus nerve, suggests that our chronic
619 VNS regime did not result in irreversible electrochemical reactions and Pt dissolution.

620

621 *Minimal off-target effects of VNS*

622 Stimulation of the vagus nerve in the lower thorax activates afferent and efferent fibers
623 which connect the brain to the gastrointestinal tract, pancreas, gallbladder and liver
624 [43]. Therefore, stimulation of the vagus nerve in the lower thorax may have effects on
625 food intake. Bilateral stimulation of the gastric vagus nerve has been shown to be
626 effective in limiting weight gain, food consumption and intake of sweet food in obese
627 mini-pigs [44]. Here, we observed no evidence of a change in eating behaviour following
628 the onset of suprathreshold VNS (note that no conclusion can be drawn on the effect of
629 VNS on increasing food intake, as sheep usually ate all the food they were given).
630 Furthermore, no significant detectable change to faecal output was seen following the
631 onset of stimulation. There were minimal effects to heart rate and respiration during
632 the onset of stimulation.

633 Any changes in heart rate and respiration patterns following the initial onset of
634 stimulation were typically not evident at later time points. The decrease in cardiac and

635 respiratory side-effects over time is probably related to the development of tissue
636 encapsulation around the electrode array reducing current spread to other structures.
637 Furthermore, since changes were small and recorded in awake animals, it is possible
638 that they indicated awareness of the stimulus rather than off-target stimulation of vagal
639 fibers controlling heart rate or respiration. In summary, chronic stimulation at levels
640 well above those required to evoke C-fiber activity produced few sustained off-target
641 effects and no measurable effects on the animal's behaviour.

642

643 *Clinical relevance*

644 For clinical application, it is anticipated that this electrode array would be placed sub-
645 diaphragmatically, onto the anterior abdominal vagus nerve above the junction of the
646 celiac and hepatic branches. As noted in the Introduction, the abdominal vagus nerve is
647 composed mainly of C-fibers that innervate visceral organs and is below branches to the
648 larynx, heart and lungs, thereby reducing any potential off-target effects experienced
649 with cervical VNS. This is supported by previous studies that found no changes to heart
650 rate during abdominal vagal nerve stimulation in pigs [45, 46]. Although abdominal
651 surgery is more invasive than cervical VN implantation surgery, laparoscopic
652 implantation of a neural stimulator around vagal gastric branches of the stomach
653 already has FDA approval for the treatment of obesity [47, 48]. We anticipate that the
654 ability to record evoked neural activity, which is a feature of this electrode array, will
655 allow for the titration of stimulus parameters so that precise stimulation levels can be
656 selected for optimal therapeutic benefit and for stimulation to be tailored to an
657 individual's specific needs.

658

659 *Study limitations*

660 Although we have shown that chronic implantation and stimulation of the anterior
661 vagus nerve is safe and feasible, we did not evaluate the efficacy of stimulating the vagus
662 nerve in the lower thorax in alleviating IBD in the present study. While the anti-
663 inflammatory mechanisms of VNS for IBD have not yet been unequivocally defined, it is
664 likely that stimulation of the vagus nerve below the branches to the larynx, heart and
665 lungs would result in similar therapeutic effects on inflammatory diseases to those seen
666 when stimulation is applied to the cervical vagus nerve [11, 12].

667

668

669 **5. Conclusion**

670 Chronic implantation and electrical stimulation using this novel vagus nerve electrode
671 array at a site below the branches to the larynx, heart and lungs, is safe and results in

672 minimal sustained off-target effects. Furthermore, the novel design of this electrode
673 array is expected to allow the titration of stimulus parameters so that precise
674 stimulation levels can be selected for optimal therapeutic benefit.

675

676

677 6. References

- 678 1. Donaldson N, Brindley GS. The historical foundations of bionics. In: *Neurobionics: The*
679 *biomedical engineering of neural prostheses*, R.K S (Ed.^(Eds).John Wiley & Sons Inc.
680 Hoboken 49-51 (2016).
- 681 2. Shepherd RK, Villalobos J, Burns O, Nayagam DA. The development of neural stimulators: A
682 review of preclinical safety and efficacy studies. *J. Neural. Eng.* 15(4), 041004 (2018).
- 683 3. Payne SC, Furness JB, Stebbing MJ. Bioelectric neuromodulation for gastrointestinal
684 disorders: effectiveness and mechanisms. *Nat. Rev. Gastroenterol. Hepatol.*
685 doi:10.1038/s41575-018-0078-6 (2018).
- 686 4. Thin NN, Horrocks EJ, Hotouras A *et al.* Systematic review of the clinical effectiveness of
687 neuromodulation in the treatment of faecal incontinence. *Br. J. Surg.* 100(11), 1430-1447
688 (2013).
- 689 5. Dinning PG, Hunt L, Patton V *et al.* Treatment efficacy of sacral nerve stimulation in slow
690 transit constipation: A two-phase, double-blind randomized controlled crossover study. *Am.*
691 *J. Gastroenterol.* 110(5), 733-740 (2015).
- 692 6. Sulkowski JP, Nacion KM, Deans KJ *et al.* Sacral nerve stimulation: A promising therapy for
693 fecal and urinary incontinence and constipation in children. *J. Pediatr. Surg.* 50(10), 1644-
694 1647 (2015).
- 695 7. Siegel SW, Catanzaro F, Dijkema HE *et al.* Long-term results of a multicenter study on sacral
696 nerve stimulation for treatment of urinary urge incontinence, urgency-frequency, and
697 retention. *Urology* 56(6 Suppl 1), 87-91 (2000).
- 698 8. Schachter SC. Vagus nerve stimulation therapy summary: Five years after FDA approval.
699 *Neurology* 59(6 Suppl 4), S15-20 (2002).
- 700 9. Nemeroff CB, Mayberg HS, Krahl SE *et al.* VNS therapy in treatment-resistant depression:
701 Clinical evidence and putative neurobiological mechanisms. *Neuropsychopharmacology*
702 31(7), 1345-1355 (2006).
- 703 10. Borovikova LV, Ivanova S, Zhang M *et al.* Vagus nerve stimulation attenuates the systemic
704 inflammatory response to endotoxin. *Nature* 405(6785), 458-462 (2000).
- 705 11. Koopman FA, Chavan SS, Miljko S *et al.* Vagus nerve stimulation inhibits cytokine production
706 and attenuates disease severity in rheumatoid arthritis. *Proc. Natl. Acad. Sci. U S A.* 113(29),
707 8284-8289 (2016).
- 708 12. Bonaz B, Sinniger V, Hoffmann D *et al.* Chronic vagus nerve stimulation in Crohn's disease: A
709 6-month follow-up pilot study. *Neurogastroenterol. Motil.* 28(6), 948-953 (2016).
- 710 13. Handforth A, Degiorgio CM, Schachter SC *et al.* Vagus nerve stimulation therapy for partial-
711 onset seizures: A randomized active-control trial. *Neurology* 51(1), 48-55 (1998).
- 712 14. Degiorgio CM, Schachter SC, Handforth A *et al.* Prospective long-term study of vagus nerve
713 stimulation for the treatment of refractory seizures. *Epilepsia* 41(9), 1195-1200 (2000).
- 714 15. Castoro MA, Yoo PB, Hincapie JG *et al.* Excitation properties of the right cervical vagus nerve
715 in adult dogs. *Exp. Neurol.* 227(1), 62-68 (2011).
- 716 16. Payne SC, Furness JB, Stebbing M. Bioelectric neuromodulation for gastrointestinal
717 disorders: effectiveness and mechanisms. *Nat Rev Gastroenterol Hepatol* In Press (2018).

- 718 17. Martelli D, Mckinley MJ, Mcallen RM. The cholinergic anti-inflammatory pathway: A critical
719 review. *Auton. Neurosci.* 182 65-69 (2014).
- 720 18. Howland RH. Vagus Nerve Stimulation. *Curr. Behav. Neurosci. Rep.* 1(2), 64-73 (2014).
- 721 19. Hoffman HH, Schnitzlein HN. The numbers of nerve fibers in the vagus nerve of man. *Anat.*
722 *Rec.* 139 429-435 (1961).
- 723 20. Tyler DJ, Durand DM. Chronic response of the rat sciatic nerve to the flat interface nerve
724 electrode. *Ann. Biomed. Eng.* 31(6), 633-642 (2003).
- 725 21. Shepherd RK, Villalobos J, Burns O, Nayagam DaX. The development of neural stimulators: a
726 review of preclinical safety and efficacy studies. *J Neural Eng* 15(4), 041004 (2018).
- 727 22. Shannon RV. A model of safe levels for electrical stimulation. *IEEE Trans. Biomed. Eng.* 39(4),
728 424-426 (1992).
- 729 23. Merrill DR, Bikson M, Jefferys JG. Electrical stimulation of excitable tissue: Design of
730 efficacious and safe protocols. *J. Neurosci. Methods* 141(2), 171-198 (2005).
- 731 24. Cogan SF, Ludwig KA, Welle CG, Takmakov P. Tissue damage thresholds during therapeutic
732 electrical stimulation. *J. Neural. Eng.* 13(2), 021001 (021013 pp) (2016).
- 733 25. McCreery D. Tissue reaction to electrodes: The problem of safe and effective stimulation of
734 neural tissue. In: *Neural Prosthesis: Theory and Practise*, Horch DS, Dhillon GS
735 (Ed.^(Eds). World Scientific Publishing River Edge, NJ (2004).
- 736 26. Langenberg C, Wan L, Egi M, May CN, Bellomo R. Renal blood flow in experimental septic
737 acute renal failure. *Kidney. Int.* 69(11), 1996-2002 (2006).
- 738 27. Fallon JB, Senn P, Thompson AC. A highly configurable neurostimulator for chronic pre-
739 clinical stimulation studies. *Neural Interfaces Conferences* (2018).
- 740 28. Patrick JF, Seligman PM, Money DK, J.A K. *Engineering in Cochlear Prostheses.* Churchill
741 Livingston, Edinburgh 99-124 (1990).
- 742 29. Richardson RT, Wise AK, Thompson BC *et al.* Polypyrrole-coated electrodes for the delivery
743 of charge and neurotrophins to cochlear neurons. *Biomaterials* 30(13), 2614-2624 (2009).
- 744 30. Villalobos J, Nayagam DA, Allen PJ *et al.* A wide-field suprachoroidal retinal prosthesis is
745 stable and well tolerated following chronic implantation. *Invest. Ophthalmol. Vis. Sci.* 54(5),
746 3751-3762 (2013).
- 747 31. Shepherd RK, Wise AK, Enke YL, Carter PM, Fallon JB. Evaluation of focused multipolar
748 stimulation for cochlear implants: A preclinical safety study. *J Neural Eng* 14(4), 046020
749 (2017).
- 750 32. Nayagam DA, Durmo I, MCGowan C, Williams RA, Shepherd RK. Techniques for processing
751 eyes implanted with a retinal prosthesis for localized histopathological analysis: Part 2
752 epiretinal implants with retinal tacks. *J. Vis. Exp.* 96 e52348 (52349 pp) (2015).
- 753 33. Clark GM, Shepherd RK, Patrick JF, Black RC, Tong YC. Design and fabrication of the banded
754 electrode array. *Ann. N. Y. Acad. Sci.* 405 191-201 (1983).
- 755 34. Tyler DJ, Durand DM. Functionally selective peripheral nerve stimulation with a flat interface
756 nerve electrode. *IEEE Trans. Neural. Syst. Rehabil. Eng.* 10(4), 294-303 (2002).
- 757 35. Schiefer MA, Polasek KH, Triolo RJ, Pinault GC, Tyler DJ. Selective stimulation of the human
758 femoral nerve with a flat interface nerve electrode. *J. Neural. Eng.* 7(2), 26006 (2010).
- 759 36. Dweiri YM, Stone MA, Tyler DJ, McCallum GA, Durand DM. Fabrication of high contact-
760 density, flat-interface nerve electrodes for recording and stimulation applications. *J Vis Exp*
761 116 e54388 (2016).
- 762 37. Tan DW, Schiefer MA, Keith MW, Anderson JR, Tyler J, Tyler DJ. A neural interface provides
763 long-term stable natural touch perception. *Sci. Transl. Med.* 6(257), 257ra138 (2014).
- 764 38. Fallon JB, Carter PM. Principles of recording from and electrical stimulation of neural tissue.
765 In: *Neurobionics: The biomedical engineering of neural prostheses*, Shepherd RK
766 (Ed.^(Eds). John Wiley & Sons, Inc. New Jersey (2016).
- 767 39. He Z, Jin Y. Intrinsic control of axon regeneration. *Neuron* 90(3), 437-451 (2016).

- 768 40. Somann JP, Albors GO, Neihouser KV *et al.* Chronic cuffing of cervical vagus nerve inhibits
769 efferent fiber integrity in rat model. *J. Neural. Eng.* 15(3), 036018 (2018).
- 770 41. Berkelaar M, Clarke DB, Wang YC, Bray GM, Aguayo AJ. Axotomy results in delayed death
771 and apoptosis of retinal ganglion cells in adult rats. *J. Neurosci.* 14(7), 4368-4374 (1994).
- 772 42. Brummer SB, Turner MJ. Electrochemical considerations for safe electrical stimulation of the
773 nervous system with platinum electrodes. *IEEE Trans. Biomed. Eng.* 24(1), 59-63 (1977).
- 774 43. Bonaz B, Picq C, Sinniger V, Mayol JF, Clarencon D. Vagus nerve stimulation: From epilepsy to
775 the cholinergic anti-inflammatory pathway. *Neurogastroenterol. Motil.* 25(3), 208-221
776 (2013).
- 777 44. Val-Laillet D, Biraben A, Randuineau G, Malbert CH. Chronic vagus nerve stimulation
778 decreased weight gain, food consumption and sweet craving in adult obese minipigs.
779 *Appetite* 55(2), 245-252 (2010).
- 780 45. Stakenborg N, Wolthuis AM, Gomez-Pinilla PJ *et al.* Abdominal vagus nerve stimulation as a
781 new therapeutic approach to prevent postoperative ileus. *Neurogastroenterol. Motil.* 29(9),
782 e13075-13086 (2017).
- 783 46. Wolthuis AM, Stakenborg N, D'hoore A, Boeckxstaens GE. The pig as preclinical model for
784 laparoscopic vagus nerve stimulation. *Int. J. Colorectal. Dis.* 31(2), 211-215 (2016).
- 785 47. Camilleri M, Toouli J, Herrera MF *et al.* Intra-abdominal vagal blocking (vBloc therapy):
786 Clinical results with a new implantable medical device. *Surgery* 143(6), 723-731 (2008).
- 787 48. Apovian CM, Shah SN, Wolfe BM *et al.* Two-year outcomes of vagal nerve blocking (vBloc)
788 for the treatment of obesity in the ReCharge trial. *Obes. Surg.* 27(1), 169-176 (2017).
- 789